ELSEVIER

Journal of Orthopaedic Research 22 (2004) 535–543

Journal of Orthopaedic Research

www.elsevier.com/locate/orthres

Self-hardening calcium phosphate composite scaffold for bone tissue engineering ☆

Hockin H.K. Xu [a,*], Carl G. Simon Jr. [b]

[a] *Paffenbarger Research Center, American Dental Association Foundation, National Institute of Standards and Technology, Building 224, Room A-153, 100 Bureau Drive Stop 8546, Gaithersburg, MD 20899, USA*

[b] *Polymers Division, National Institute of Standards and Technology, Gaithersburg, MD 20899, USA*

Received 12 September 2003; accepted 12 September 2003

Abstract

Calcium phosphate cement (CPC) sets in situ to form solid hydroxyapatite, can conform to complex cavity shapes without machining, has excellent osteoconductivity, and is able to be resorbed and replaced by new bone. Therefore, CPC is promising for craniofacial and orthopaedic repairs. However, its low strength and lack of macroporosity limit its use. This study investigated CPC reinforcement with absorbable fibers, the effects of fiber volume fraction on mechanical properties and macroporosity, and the cytotoxicity of CPC–fiber composite. The rationale was that large-diameter absorbable fibers would initially strengthen the CPC graft, then dissolve to form long cylindrical macropores for colonization by osteoblasts. Flexural strength, work-of-fracture (toughness), and elastic modulus were measured vs. fiber volume fraction from 0% (CPC Control without fibers) to 60%. Cell culture was performed with osteoblast-like cells, and cell viability was quantified using an enzymatic assay. Flexural strength (mean ± SD; $n = 6$) of CPC with 60% fibers was 13.5 ± 4.4 MPa, three times higher than 3.9 ± 0.5 MPa of CPC Control. Work-of-fracture was increased by 182 times. Long cylindrical macropores 293 ± 46 μm in diameter were created in CPC after fiber dissolution, and the CPC–fiber scaffold reached a macroporosity of 55% and a total porosity of 81%. The new CPC–fiber formulation supported cell adhesion, proliferation and viability. The method of using large-diameter absorbable fibers in bone graft for mechanical properties and formation of long cylindrical macropores for bone ingrowth may be applicable to other tissue engineering materials.
Published by Elsevier Ltd. on behalf of Orthopaedic Research Society.

Keywords: Calcium phosphate scaffold; Hydroxyapatite; Absorbable fiber reinforcement; Cell culture; Tissue engineering

Introduction

The need for biomaterials has increased as the world population ages [16,25,37]. Bone grafts have been used for decades to repair osseous defects resulting from trauma and disease and over 800,000 grafting procedures are performed each year [25]. Hydroxyapatite is an important biomaterial for hard tissue repair because of its chemical and crystallographic similarity to the carbonated apatite in teeth and bones [16,18,37]. Several calcium phosphate cements (CPCs) self-harden to form hydroxyapatite [5,8,14,29]. One calcium phosphate cement (referred to as CPC) is comprised of tetracalcium phosphate and dicalcium phosphate anhydrous and forms hydroxyapatite as the only final product [5].

The CPC powder can be mixed with water to form a thick paste that can be sculpted during surgery to conform to the defects in hard tissues, and then sets in situ to form hydroxyapatite [7]. A major disadvantage of current orthopaedic implant materials is that they exist in a hardened form, requiring the surgeon to fit the surgical site around the implant or to carve the graft to the desired shape. This can lead to increases in bone loss, trauma to the surrounding tissue, and surgical time [25]. Therefore, CPC's moldability and in situ self-hardening ability, together with its excellent osteoconductivity, make it a highly desirable material for orthopaedic repair. CPC has been investigated for use in the reconstruction of frontal sinus, augmentation of craniofacial skeletal defects, endodontics and periodontal bone repair [9,13,38]. However, due to its low strength, the use of CPC was "limited to the reconstruction of

☆ Official contribution of the National Institute of Standards and Technology; not subject to Copyright in the United States.

* Corresponding author. Tel.: +1-301-975-6804; fax: +1-301-963-9143.

E-mail address: hockin.xu@nist.gov (H.H.K. Xu).

0736-0266/$ - see front matter Published by Elsevier Ltd. on behalf of Orthopaedic Research Society.
doi:10.1016/j.orthres.2003.09.010

non-stress-bearing bone" [9], and "clinical usage was limited by... brittleness..." [13]. In periodontal bone repair, tooth mobility resulted in the early fracture and eventual exfoliation of the brittle CPC implants [4].

The fracture resistance of biomaterials can be improved via fiber reinforcement [15,22,23,32,42–44]. Recent studies incorporated a variety of fibers into CPC and substantially increased the strength and fracture resistance [46,49]. One study [11] incorporated polyamide fibers into a CPC based on alpha-tricalcium phosphate. Another study used a mesh on the tensile side of CPC to increase the work-to-fracture [45]. Macropores were built into implants to facilitate cell infiltration, tissue ingrowth, and implant fixation [3,6,17,18,20,24, 26–28,30]. Our recent studies incorporated a variety of fibers, as well as water-soluble porogens, into CPC to obtain strength as well as macropores for bone ingrowth [46,49]. In another study, we reinforced CPC with absorbable fibers that provided the needed early strength and then dissolved to create macropores for tissue ingrowth [47]. That study used only a single volume fraction of absorbable fibers, without investigating the effects of fiber volume fraction on mechanical properties and macropore volume fraction [47]. Furthermore, the cytotoxicity of the new CPC–fiber composite was not examined.

The present study investigated the effects of absorbable fiber volume fraction on CPC composite mechanical properties and macroporosity of the scaffold after fiber dissolution, and examined the cytotoxicity of the new CPC–fiber composite. The rationale for the microstructural design was that large-diameter absorbable fibers would initially strengthen and toughen the graft, then dissolve to form long cylindrical macropores for colonization by osteoblasts. It was hypothesized that increasing the absorbable fiber volume fraction would significantly increase the initial composite strength and then the macropore volume fraction, and the new CPC–fiber composition would be non-cytotoxic.

Methods

Specimens for mechanical properties and density

CPC powder consisted of a mixture of tetracalcium phosphate (TTCP: $Ca_4[PO_4]_2O$) and dicalcium phosphate anhydrous (DCPA: $CaHPO_4$), with a TTCP:DCPA molar ratio of 1. TTCP powder was synthesized from a solid-state reaction between $CaHPO_4$ and $CaCO_3$ (Baker Chemical Company, NJ), then ground and sieved to obtain TTCP particle sizes of 1–80 μm, with a median particle size of 17 μm. The DCPA powder was ground and sieved to obtain particle sizes of 0.4–3 μm, with a median particle size of 1 μm. The TTCP and DCPA powders were then mixed in a blender (Dynamics Corporation of America, New Hartford, CT) to form the CPC powder.

An absorbable suture fiber (Vicryl, Ethicon, Somerville, NJ) was used because this type of fiber is clinically used as sutures, and it possessed a relatively high strength [46]. This suture consisted of individual fibers braided into a bundle with a diameter of 322 μm, provided substantial strength and toughness for about four weeks, and then dissolved and produced macropores as shown in a previous study [47]. As in that study, the suture was cut to filaments of 8 mm in length. CPC powder was mixed with distilled water at a powder: liquid mass ratio of 2:1 to form a flowable paste suitable for the incorporation of a relatively large amount of fibers for increased mechanical properties. The filaments were mixed with the CPC paste randomly to form a composite paste, which was placed into a rectangular mold of $3\times4\times25$ mm^3 and set in a humidor with 100% relative humidity for 4 h at 37 °C [47]. Fiber volume fractions of 0%, 15%, 30%, 45% and 60% were used, calculated using fiber density and specimen volume [47]. For flexural testing, the bar specimens were immersed in a physiological solution (1.15 mmol/l Ca, 1.2 mmol/l P, 133 mmol/l NaCl, 50 mmol/l Hepes [*N*-2-hydroxyethyl-piperazine-*N*′-2′-ethane sulfonic acid], buffered to 7.4 pH) at 37 °C for 20 h prior to testing [48]. For density measurement, bar specimens were immersed for 17 weeks (119 d). Preliminary studies showed that it took this time to dissolve this batch of absorbable fibers and create macropores inside the CPC bulk.

Mechanical testing and density measurement

A standard three-point flexural test [1] with 20 mm span was used to fracture the specimens at a crosshead speed of 1 mm/min on a Universal Testing Machine (model 5500R, Instron, MA). After taking the specimen out of the physiological solution, the 4×25 mm^2 side of the specimen was consecutively polished in water with SiC papers of 400, 600, and 1200 grits. Within about half an hour, the specimen was tested in air by placing the polished surface in tension. Flexural strength, elastic modulus, and work-of-fracture (toughness) were measured [46]. For CPC–fiber specimens that did not fail catastrophically, the test was stopped at a displacement of 3 mm for a consistent calculation of work-of-fracture. In comparison, CPC specimens without fibers failed catastrophically at a displacement of approximately 0.045 mm.

To measure density, specimens immersed for 119 d were dried in a vacuum oven at 60 °C for 24 h. The density was measured using the specimen weight divided by the specimen volume. As in a previous study [49], the specimen volume was calculated by the specimen dimensions measured with a micrometer, with each linear dimension the average of three locations along the specimen. Six specimens were measured at each of the five fiber volume fractions used.

CPC contains micrometer-sized micropores after forming hydroxyapatite [7]. The total porosity including the intrinsic micropores and macropores from fiber dissolution, P_{TOTAL}, can be obtained by

$$P_{TOTAL} = (d_{HA} - d)/d_{HA} \quad (1)$$

where d_{HA} is the density of fully dense hydroxyapatite (3.14 g/cm^3) [39], and d is the measured density. The macroporosity, P_{MACRO}, can then be calculated. The total volume of a specimen is

$$V = V_{MACRO} + V_{MATRIX} \quad (2)$$

where V_{MACRO} is the macropore volume in the specimen, and V_{MATRIX} is the rest of the specimen. Dividing Eq. (2) by V gives the macroporosity

$$P_{MACRO} = V_{MACRO}/V = 1 - V_{MATRIX}/V \quad (3)$$

or

$$P_{MACRO} = 1 - (V_{MATRIX}/V)(W/W) \quad (4)$$

where W is the mass of specimen. W/V equals the measured density of the specimen, d. W/V_{MATRIX} equals the density of CPC with 0% fiber, $d_{0\%Fiber}$. Therefore, the macroporosity in CPC

$$P_{MACRO} = 1 - d/d_{0\%Fiber} \quad (5)$$

Thus the macroporosity of CPC at a particular fiber volume fraction can be calculated by using the measured density d of the specimen at that fiber volume fraction.

Cell culture specimens

Because cell culture toxicity assays are the international standard for cytotoxicity screening [19], in vitro cell culture was performed to evaluate the cytotoxicity of the new cement formulation. The same CPC powder to liquid ratio and the same fibers with 60% volume fraction were used as described above, and the paste was placed in a

disc mold with 10 mm diameter and 4 mm height. Specimens were set in a cell incubator at 100% relative humidity and 37 °C for 24 h. Eighteen CPC–fiber discs and 18 CPC Control discs were made and divided into three groups, with six discs of each material in each group. These three groups were used for 1 d cell culture, 14 d cell culture, and an enzymatic assay, respectively.

Cell culture and fluorescence microscopy

MC3T3-E1 osteoblast-like cells (Riken, Hirosaka, Japan) were cultured following established protocols [2,34]. Cells were cultured in flasks at 37 °C and 100% humidity with 5% CO_2 (volume fraction) in α modified Eagle's minimum essential medium (Biowhittaker, Walkersville, MD). The medium was supplemented with 10% volume fraction of fetal bovine serum (Gibco, Rockville, MD) and kanamycin sulfate (Sigma, St. Louis, MO), and changed twice weekly. The cultures were passaged with 2.5 g/l trypsin containing 1 mmol/l EDTA (Gibco, Rockville, MD) once per week. Cultures of 90% confluent cells were trypsinized, washed and suspended in fresh media. Fifty thousand cells diluted into 2 ml of media were added to each well containing a specimen or to an empty well of tissue culture polystyrene (TCPS), and incubated for 1 d or 14 d (2 ml of fresh media every 2 d) [34].

After 1 d or 14 d incubations of the cells on the CPC–fiber, CPC Control or TCPS, the media was removed and the cells were washed two times in 2 ml of Tyrode's Hepes buffer (140 mmol/l NaCl, 0.34 mmol/l Na_2HPO_4, 2.9 mmol/l KCl, 10 mmol/l Hepes, 12 mmol/l $NaHCO_3$, 5 mmol/l glucose, pH 7.4). Cells were then stained and viewed by epifluorescence microscopy (Eclipse TE300, Nikon, Melville, NY). Staining of cells was done for 1 h with 2 ml of Tyrode's Hepes buffer containing 2 μmol/l calcein-AM and 2 μmol/l ethidium homodimer-1 (both from Molecular Probes, Eugene, OR). Calcein-AM is a non-fluorescent, cell-permeant fluorescein derivative, which is converted by cellular enzymes into cell-impermeant and highly fluorescent calcein. Calcein accumulates inside live cells having intact membranes causing them to fluoresce green. Ethidium-homodimer-1 enters dead cells with damaged membranes and undergoes a 40-fold enhancement of fluorescence upon binding to their DNA causing the nuclei of dead cells to fluoresce red. Double-staining cells anchored on the bone graft discs allows simultaneous examination of both live and dead cells on the discs.

Wst-1 cell viability assay

Wst-1 measures mitochondrial dehydrogenase activity [21] and refers to 2-(4-iodophenyl)-3-(4-nitrophenyl)-5-(2,4-disulfophenyl)-2H-tetrazolium, monosodium salt (Dojindo, Gaithersburg, MD). At 14 d, specimens with cells were transferred to wells in a 24-well plate and rinsed with 1 ml of Tyrode's Hepes buffer. One milliliters of Tyrode's Hepes buffer and 0.1 ml of Wst-1 solution (5 mmol/l Wst-1 and 0.2 mmol/l 1-methoxy-5-methylphenazinium methylsulfate in water) were added to each well and incubated at 37 °C for 2 h. Then 200 μl of each reaction mixture was transferred to a 96-well plate and the absorbance at 450 nm was measured with a microplate reader (Wallac 1420 Victor^2, PerkinElmer Life Sciences, Gaithersburg, MD).

Scanning electron microscopy

A scanning electron microscope (SEM, JEOL 5300, Peabody, MA) was used to examine the CPC composite specimens and the cells on the specimens. Cells cultured for 1 d on specimens were rinsed with saline, fixed with 1% glutaraldehyde, subjected to graded alcohol dehydrations, rinsed with hexamethyldisilazane, and then sputter coated with gold.

Statistics

One standard deviation was used as the estimated standard uncertainty of the measurements. These values should not be compared with data obtained in other laboratories under different conditions. One-way ANOVA was performed to detect significant effects. Tukey's multiple comparison procedures were used to compare the data at a family confidence coefficient of 0.95.

Results

Mechanical properties

As shown in Fig. 1, fiber volume fraction had significant effects ($p < 0.001$; one-way ANOVA) on strength and work-of-fracture, but not on modulus ($p = 0.073$).

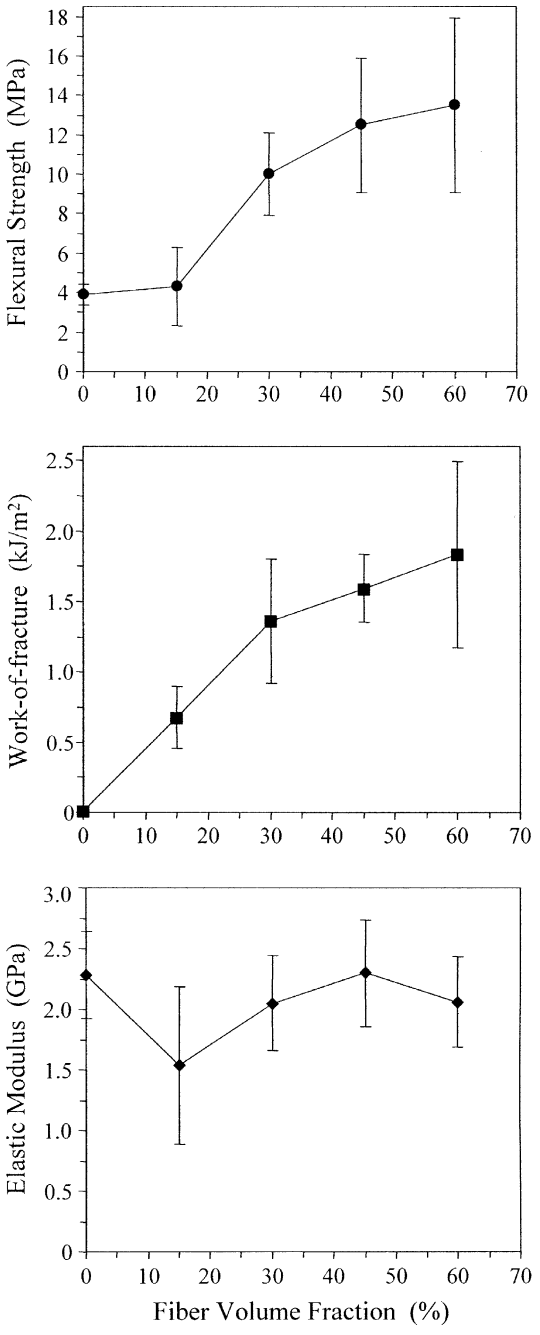

Fig. 1. Flexural strength, work-of-fracture and elastic modulus vs. fiber volume fraction of CPC composites after immersion in a physiological solution for 1 d. Each value is the mean of six repeats, with the error bar showing one standard deviation (mean ± SD; $n = 6$). Lines connect data points.

The strength (mean ± SD; $n = 6$) of CPC Control with 0% fibers was 3.9 ± 0.5 MPa; that of CPC containing 60% fibers was increased to 13.5 ± 4.4 MPa. The strengths at 0% and 15% fibers were not significantly different (Tukey's multiple comparison test; family confidence coefficient = 0.95). Work-of-fracture at 60% fibers was 1.83 ± 0.66 kJ/m^2, an increase of two orders of magnitude over 0.010 ± 0.001 kJ/m^2 of CPC Control.

Specimen density

After macropore formation in immersion in a physiological solution for 17 weeks, specimen bulk density was measured (mean ± SD; $n = 6$). For CPC with 0%, 15%, 30%, 45% and 60% of fibers, the density was 1.31 ± 0.01 g/cm^3, 1.09 ± 0.06 g/cm^3, 0.92 ± 0.02 g/cm^3, 0.75 ± 0.07 g/cm^3 and 0.59 ± 0.03 g/cm^3, respectively. All of these values were significantly different from each other (Tukey's multiple comparison test; $p < 0.001$).

Macroporosity

Macropores were formed in CPC from fiber dissolution throughout the 3×4×25 mm^3 specimen after immersion for 17 weeks (Fig. 2(A)). The two long arrows indicate macropore channels that went into the bulk of the specimen. The short arrow points to grooves formed by the imprints of the individual fibers in the braided bundle, indicating good wetting of the fibers by the CPC paste. Fig. 2(B) shows specimen with perpendicular macropores that were empty. An example of pores that were not completely empty is shown in Fig. 2(C); such a pore structure indicates that the outer layer of fibers in the suture bundle were mingled with the CPC paste during mixing. The macropore diameter was measured with SEM for 50 randomly selected macropores (mean ± SD; $n = 50$) to be 293 ± 46 μm. The diameter of the suture bundle was measured in a previous study to be 322 ± 13 μm [47]. These two values are not significantly different (Student's t test; $p > 0.1$).

Fig. 3 plots total porosity of CPC scaffold from Eq. (1) and macroporosity of CPC scaffold from equation (5). For CPC with 0%, 15%, 30%, 45% and 60% of fibers, the macroporosity P_{MACRO} after fiber dissolution was 0%, 16.8 ± 5.2%, 30.0 ± 2.3%, 42.7 ± 5.8% and 55.0 ± 2.8%, respectively. The total porosity P_{TOTAL} reached 81.2 ± 1.0% for the CPC scaffold that had a fiber volume fraction of 60%.

Cell adhesion

Cells cultured for 1 d are shown in Fig. 4: (A) live cells on CPC–fiber, (B) dead cells on CPC–fiber, (C) live cells on CPC Control, (D) live cells on TCPS Control. Live cells (stained green) appeared to have adhered and attained a normal, polygonal morphology on all materials. Visual examination revealed that the density of live cells adherent to each material was similar. Dead cells (stained red) were very few on CPC–fiber, as well as on CPC Control and TCPS. The SEM micrograph in (E) shows cells with long cytoplasmic processes that attached to the surface of CPC Control. The cytoplasmic processes or extensions were observed in the SEM to have lengths ranging from about 20 to 60 μm. These are regions of the cell plasma membrane that contain a

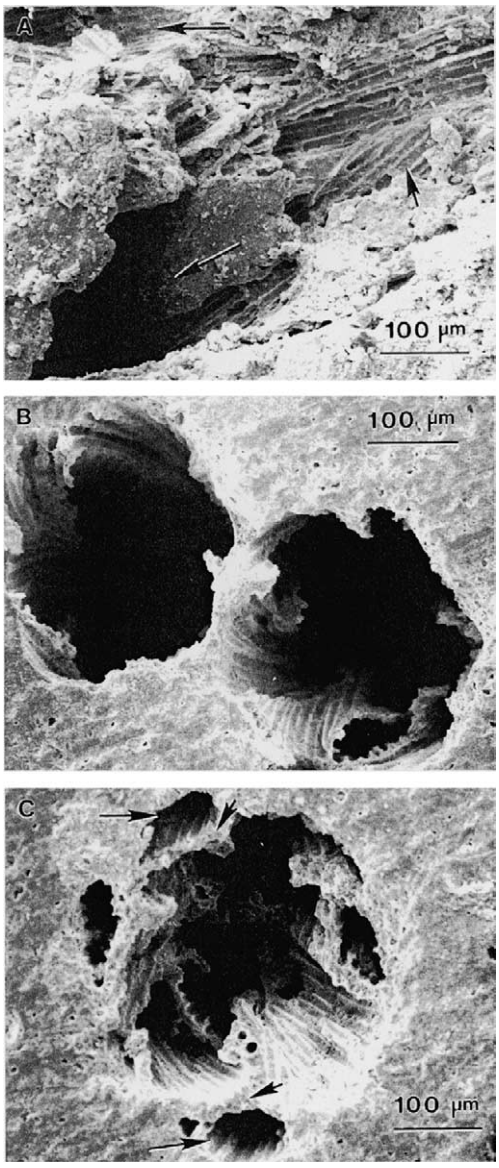

Fig. 2. Macropores in CPC after fiber dissolution in immersion in a physiological solution for 17 weeks. (A) Pores nearly parallel to the surface of a specimen with 60% fibers. Long arrows indicate macropore channels. Short arrow points to imprints of individual fibers in the braided bundle, indicating wetting of fibers by the CPC paste, (B) pores perpendicular to specimen surface that were completely empty, (C) pores that were not completely empty, where a large pore is surrounded by small pores (long arrows), separated by thin walls of CPC (short arrows).

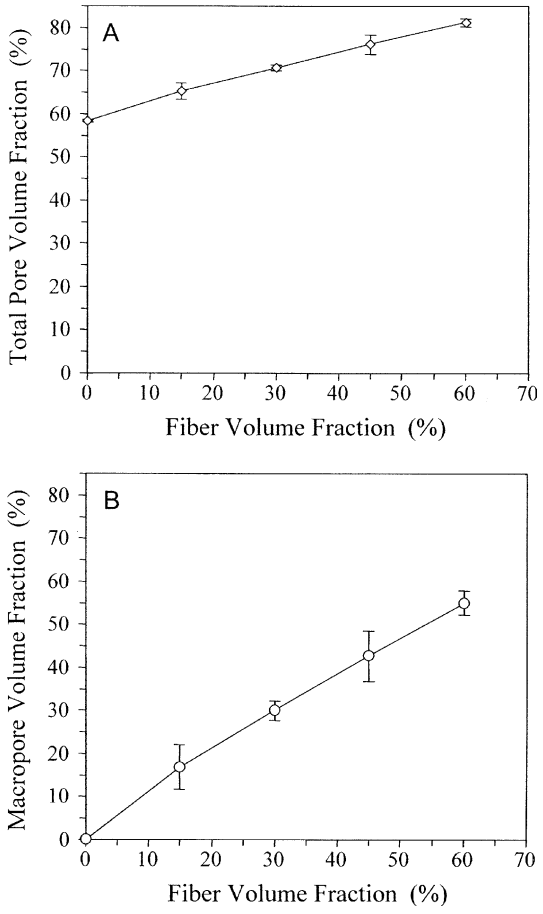

Fig. 3. (A) Total porosity in CPC scaffold, P_{TOTAL} from Eq. (1), (B) macroporosity in CPC scaffold from fiber dissolution, P_{MACRO} from Eq. (5). Each value is the mean of six repeats, with the error bar showing one standard deviation. Lines connect data points. The CPC scaffold reached a macropore volume fraction of (55.0 ± 2.8)% and a total pore volume fraction of (81.2 ± 1.0)%.

meshwork or bundles of actin-containing microfilaments, which permit the movement of the migrating cells along a substratum [10]. The similar morphologies observed on the three different materials, together with very few dead cells suggest that cell adhesion and viability on CPC–fiber was the same as that on CPC Control and TCPS Control.

Cell proliferation

Cells cultured for 14 d are shown in Fig. 5: (A) live cells (stained green) on CPC–fiber, (B) dead cells (stained red) on CPC–fiber, (C) live cells on CPC Control, (D) live cells on TCPS Control. At 14 d, live cells had formed a confluent monolayer on the discs. The 14 d live cell density was much greater than the 1 d density (Fig. 4), indicating that the cells had greatly proliferated. The live cell density appeared similar on the three materials. Dead cells were very few on CPC–fiber, as well as on CPC Control and TCPS. These results suggest that cell proliferation and viability were similar, demonstrating that CPC–fiber composite was as non-cytotoxic as CPC Control and TCPS Control.

Cell viability quantification

The viability of cells cultured for two weeks on CPC–fiber and CPC Control was quantitatively assessed with the colorimetric Wst-1 assay which measures mitochondrial dehydrogenase activity. The results are plotted in Fig. 5(E). TCPS was not included since the growth area of the 24-well TCPS plates was larger than the cement discs and hence would not allow an accurate comparison. The absorbance at 450 nm, which is proportional to the amount of dehydrogenase activity in the cells, was measured (mean ± SD; $n = 6$) to be 1.00 ± 0.28 for CPC Control and 0.82 ± 0.41 for CPC–fiber, normalized to be 1 for CPC Control. These two values are statistically similar (Student's t; $p > 0.1$), showing that similar cell dehydrogenase activity was present. Hence cell viability was quantitatively similar for CPC–fiber and CPC Control without fibers.

Discussion

Increasing the volume fraction of absorbable fibers substantially increased the strength and toughness of a hydroxyapatite cement. Compared to CPC without fibers, the strength of CPC–fiber composite more than doubled at 30% volume fraction of fibers and more than tripled at 60% fibers. Work-of-fracture (toughness) was increased by two orders of magnitude. A previous study [47] used this type of absorbable fiber in CPC and showed that the reinforcement was maintained for four weeks in a physiological solution; the strength then quickly decreased and became diminished during further immersion leading to macropore formation in CPC. That study used a single fiber volume fraction of 30%. The present study not only improved the cement mechanical properties by increasing the fiber volume fraction to 60%, but also created higher macroporosity in CPC.

One issue that needs to be further addressed is that the implant's strength may decrease when the fibers dissolve. It is possible that when implanted in vivo, the strengthening of the graft from bone ingrowth may offset the weakening of the graft due to fiber dissolution [18,31,40]. For example, the flexural strength of available sintered porous hydroxyapatite implants ranged from 2 to 11 MPa; it then increased when new bone grew into the macropores of the hydroxyapatite implants, reaching 40–60 MPa [37]. Alternatively, to achieve a gradual load-sharing transfer, fibers and fillers of different dissolution rates could be combined in the self-hardening and resorbable apatite scaffold, with fast-dissolution fillers to

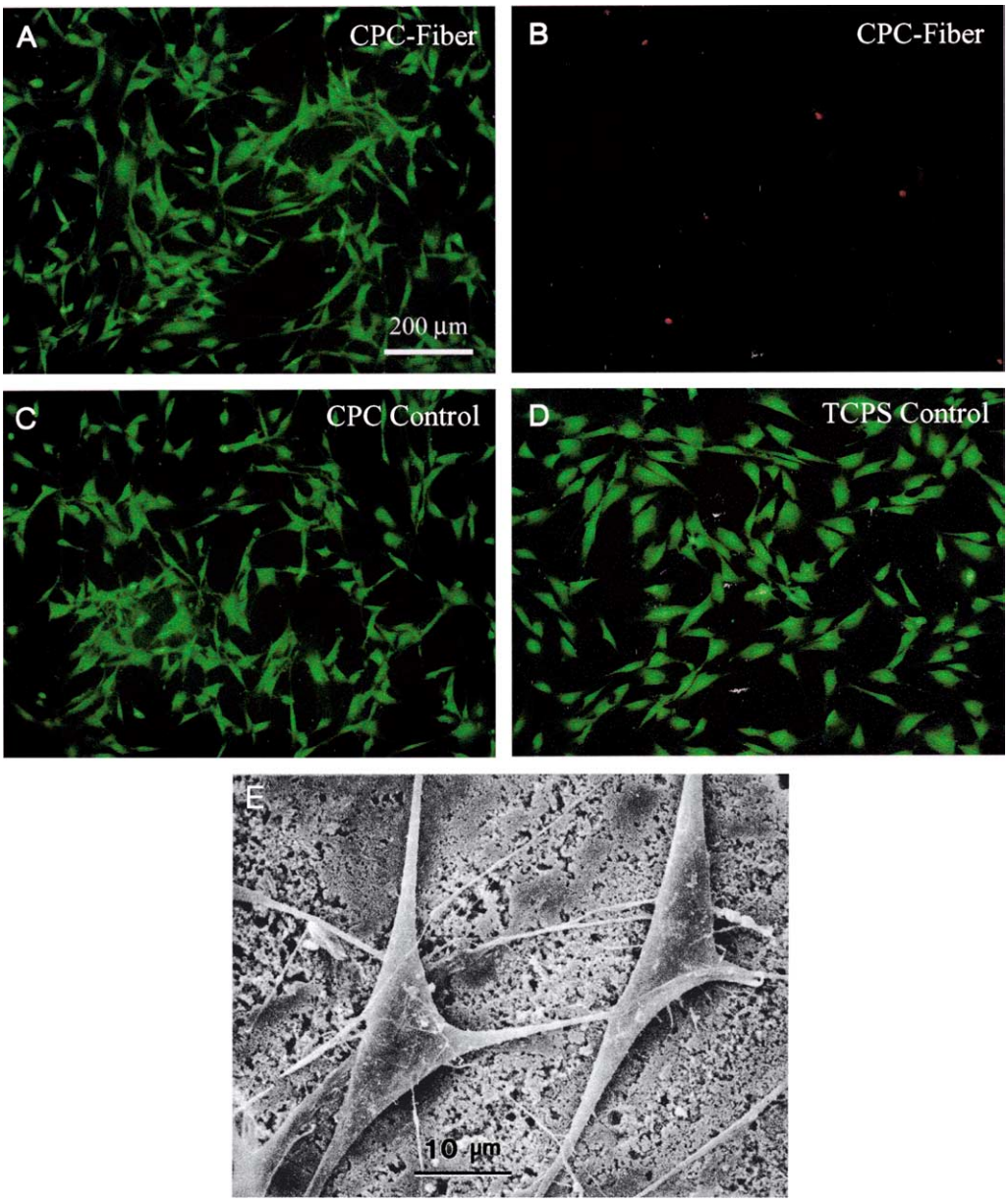

Fig. 4. Cells cultured for 1 d: (A) live cells (stained green) on CPC–fiber composite, (B) dead cells (stained red) on CPC–fiber composite, (C) live cells on CPC Control, (D) live cells on TCPS Control. The live cells appeared to have adhered and attained a normal, polygonal morphology on all three materials. Few dead cells were visible on CPC Control and TCPS Control, similar to (B) for CPC–fiber, (E) SEM of cells with long cytoplasmic processes and extensions that were attached to the surface of a CPC Control specimen, similar to those on CPC–fiber and TCPS Control specimens.

dissolve in a couple of days upon contact with the physiological solution in vivo to immediately create macropores for bone ingrowth. Meanwhile, slow-dissolution fibers would provide superior reinforcement for about 4 to 6 weeks, by which time new bone should have grown significantly into the macropores from the fast-dissolution fillers. (Previous studies observed significant bone ingrowth into porous hydroxyapatite implants at 6 weeks [40].) After significant bone ingrowth, thus increasing the implant strength, the slow-dissolution fibers would then dissolve to create additional macropores for further bone ingrowth.

The size of the mouse MC3T3-E1 osteoblast cells (Fig. 4(E)) with cytoplasmic extensions ranged from about 20 to 60 μm. The size of osteoblast cells in humans ranged from about 10 to 50 μm [36]. This is consistent with previous studies showing that macropore sizes of at least 100 μm were required for cell infiltration and bone ingrowth [35]. The inherent micropores in CPC had sizes of submicron to a few microns; examples of micropores can be seen in Fig. 4(C) of Ref. [47]. Hence these pores were too small for infiltration by the osteoblast cells. The CPC scaffolds produced in the present study were highly macroporous after fiber dissolution, with total

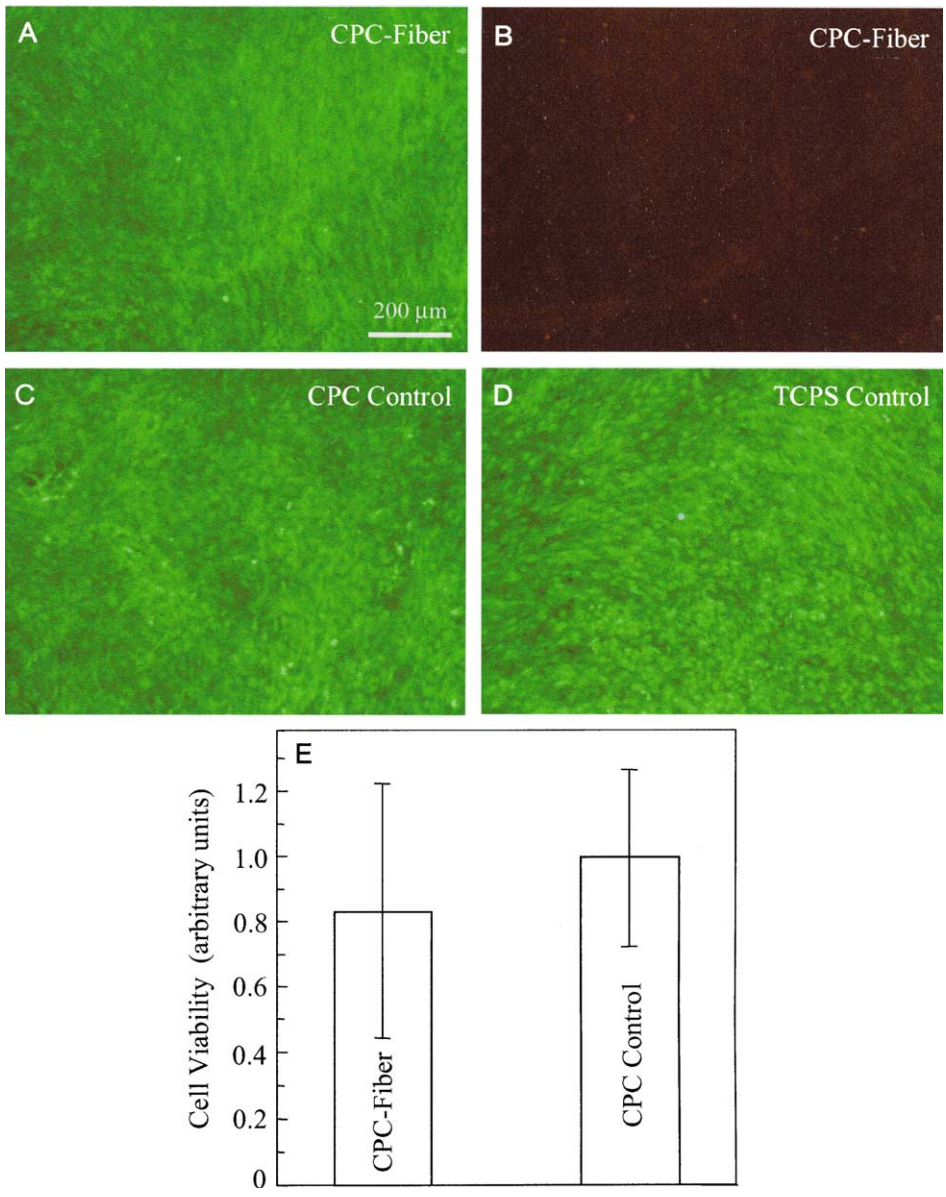

Fig. 5. Cells cultured for 14 d: (A) live cells (stained green) on CPC–fiber, (B) dead cells (stained red) on CPC–fiber, (C) live cells on CPC Control, (D) live cells on TCPS Control. Live cells formed a confluent monolayer. The live cell density appeared similar on the three materials with few dead cells, demonstrating that cells proliferated equally well on these three materials, (E) using the Wst-1 assay, cell viability at 14 d was quantified for CPC–fiber and CPC Control. TCPS was not included because it had a larger growth area than the cement discs and would not allow an accurate comparison. The absorbance at 450 nm, proportional to the amount of dehydrogenase activity in the cells, was measured and the two values are statistically similar (Student's t; $p > 0.1$).

porosity reaching 81% and macroporosity reaching 55%. The macropores in CPC were long and cylindrical with a mean diameter of 293 μm. The macropore volume fractions were consistent with the fiber volume fractions incorporated into CPC. At higher fiber volume fractions, the slightly less macropore volume fraction than fiber volume fraction (*e.g.*, a fiber volume fraction of 60% and a corresponding macropore volume fraction of 55%) may be because some fibers were sticking out of the specimen edges and did not contribute to macropore formation inside CPC.

Pore interconnection is a limiting factor for bone ingrowth, because interconnecting fenestrations that are too small would not permit cell migration or tissue invasion from pore to pore [6]. For example, one study [40] showed that a commercial porous hydroxyapatite had sufficient pore sizes of 50–300 μm; however, the pore interconnection diameters were only 0.1–2 μm. As a result, the graft exhibited poor invasion of bone tissue into the implant [40]. In the present study using 8 mm sutures, each cylindrical pore channel would be about 8 mm long. Such a single cylindrical pore would be

equivalent to nearly 27 spherical pores of 293 μm in diameter that were completely interconnected. In reality, spherical or random pores are not completely interconnected. Therefore, the long cylindrical macropores in the novel CPC scaffold should be beneficial for bone ingrowth. Furthermore, the CPC scaffold is advantageous over sintered hydroxyapatite implants, because CPC can self-harden in situ and conform to complex cavity shapes, while sintered hydroxyapatite requires machining which is difficult due to its brittleness. In addition, CPC can be resorbed and replaced by new bone [9,12,33], while sintered hydroxyapatite remains more stable.

The CPC–fiber composite bone graft was shown to be non-cytotoxic in the cell culture studies. After 1 d incubation, the osteoblast cells (MC3T3-E1) were able to adhere, spread and remain viable on CPC–fiber, CPC Control and TCPS when observed by fluorescence microscopy. After 14 d cultures, fluorescence microscopy and the quantitative Wst-1 assay showed that cell adhesion, proliferation and viability were equivalent on these materials. Therefore, these in vitro cell culture results suggest that the new CPC–fiber composite is non-cytotoxic. It should be noted that the 14 d cultures were completed before the Vicryl fibers had completely dissolved. It has been shown that most of the toxic effect of PLA and PGA occurs after 10 d [41]. Therefore, whether or not the CPC–fiber composite is non-cytotoxic after 14 d remains to be examined.

In conclusion, this study imparted substantial reinforcement and macroporosity to a moldable, self-setting and resorbable hydroxyapatite cement. The initial strength of the composite was threefold higher than that of the unreinforced CPC Control. The new CPC–fiber formulation was non-cytotoxic and supported the adhesion, spreading, proliferation and viability of osteoblast-like cells. The CPC–fiber paste could be directly applied to fit various types of bone defects. When implanted in vivo, the fibers would provide strength and then dissolve to form macropores. The strengthening of CPC from new bone ingrowth should offset the weakening of CPC due to fiber degradation. Further studies could combine porogens and fibers of different dissolution rates to form CPC scaffolds with sustained strength. One porogen in CPC could quickly dissolve and create macropores to start the bone ingrowth process, while a second type of fibers provided the needed strength to the implant. After significant bone ingrowth into the initial pores increased the implant strength, the second set of fibers would then dissolve to create additional macropores for bone ingrowth. The novel self-hardening CPC scaffolds with high strength may be useful in periodontal bone repair, mandibular and maxillary ridge augmentation, reconstruction of the frontal sinus, augmentation of craniofacial defects, and other orthopaedic repairs. The method of using large-diameter absorbable fibers in grafts for strength and then formation of long cylindrical macropores for bone ingrowth may have wide applicability to other tissue engineering materials.

Disclaimer

Certain commercial materials and equipment are identified in this paper to specify experimental procedures. In no instance does such identification imply recommendation by NIST or the ADA Health Foundation or that the material identified is necessarily the best available for the purpose.

Acknowledgements

The authors are grateful to A.A. Giuseppetti for experimental assistance, and Drs. F.C. Eichmiller, G.E. Schumacher, S. Takagi, L.C. Chow for discussions. This study was supported by NIH NIDCR grants R29 DE12476 (Xu) and R01 DE14190 (Xu), NIST, and the ADAHF.

References

[1] American Society for Testing and Materials. ASTM F417-78. Standard test method for flexural strength of electrical grade ceramics. Philadelphia: ASTM; 1984.
[2] Attawia MA, Uhrich KE, Botchwey E, Langer R, Laurencin CT. In vitro bone biocompatibility of poly(anhydride-*co*-imides) containing pyromellitylimidoalanine. J Orthop Res 1996;14:445–54.
[3] Borden M, Attawia M, Laurencin CT. The sintered microsphere matrix for bone tissue engineering: in vitro osteoconductivity studies. J Biomed Mater Res 2002;61:421–9.
[4] Brown GD, Mealey BL, Nummikoski PV, Bifano SL, Waldrop TC. Hydroxyapatite cement implant for regeneration of periodontal osseous defects in humans. J Periodont 1998;69:146–57.
[5] Brown WE, Chow LC. A new calcium phosphate water setting cement. In: Brown PW, editor. Cements research progress. Westerville, OH: American Ceramic Society; 1986. p. 352–79.
[6] Chang BS, Lee CK, Hong KS, Youn HJ, Ryu HS, Chung SS, et al. Osteoconduction at porous hydroxyapatite with various pore configurations. Biomaterials 2000;21:1291–8.
[7] Chow LC. Calcium phosphate cements: chemistry, properties, and applications. Mat Res Symp Proc 2000;599:27–37.
[8] Constantz BR, Barr BM, Ison IC, Fulmer MT, Baker J, McKinney L, et al. Histological, chemical, and crystallographic analysis of four calcium phosphate cements in different rabbit osseous sites. J Biomed Mater Res (Appl Biomater) 1998;43:451–61.
[9] Costantino PD, Friedman CD, Jones K, Chow LC, Sisson GA. Experimental hydroxyapatite cement cranioplasty. Plast Reconstr Surg 1992;90:174–91.
[10] Darnell J, Lodish H, Baltimore D. Molecular cell biology. 2nd ed. New York: Freeman and Company; 1990. p. 890–1.
[11] dos Santos LA, de Oliveira LC, da Silva Rigo EC, Carrodeguas RG, Boschi AO, Fonseca de Arruda AC. Fiber reinforced calcium phosphate cement. Artif Organs 2000;24:212–6.

[12] Friedman CD, Costantino PD, Jones K, Chow LC, Pelzer HJ, Sisson GA. Hydroxyapatite cement: II. Obliteration and reconstruction of the cat frontal sinus. Arch Otolaryngol Head Neck Surg 1991;117:385–9.
[13] Friedman CD, Costantino PD, Takagi S, Chow LC. BoneSource™ hydroxyapatite cement: a novel biomaterial for craniofacial skeletal tissue engineering and reconstruction. J Biomed Mater Res (Appl Biomater) 1998;43:428–32.
[14] Ginebra MP, Fernandez E, De Maeyer EAP, Verbeeck RMH, Boltong MG, Ginebra J, et al. Setting reaction and hardening of an apatite calcium phosphate cement. J Dent Res 1997;76:905–12.
[15] Goldberg AJ, Burstone CJ, Hadjinikolaou I, Jancar J. Screening of matrices and fibers for reinforced thermoplastics intended for dental applications. J Biomed Mater Res 1994;28:167–73.
[16] Hench LL. Bioceramics. J Am Ceram Soc 1998;81:1705–28.
[17] Hollinger JO. Animal models for assessing bone repair with emphasis on poly(-hydroxy acid) delivery systems. In: Brighton CT, Friedlaender GE, Lane JM, editors. Bone formation and repair. Rosemont, IL: American Academy of Orthopaedic Surgeons; 1994. p. 155–6.
[18] Holmes R, Mooney V, Bucholz R, Tencer A. A coralline hydroxyapatite bone graft substitute. Clin Orthop 1984;188:252–62.
[19] International Standards Organization. ISO 10993-5. Biological evaluation of medical devices—Part 5: Tests for in vitro cytotoxicity, 1999.
[20] Ishaug SL, Crane GM, Miller MJ, Yasko AW, Yaszemski MJ, Mikos AG. Bone formation by three-dimensional stromal osteoblast culture in biodegradable polymer scaffolds. J Biomed Mater Res 1997;36:17–28.
[21] Ishiyama M, Shiga M, Sasamoto K, Mizoguchi M, He P-G. A new sulfonated tetrazolium salt that produces a highly water-soluble formazan dye. Chem Pharm Bull 1993;41:1118–22.
[22] Kettunen J, Makela A, Miettinen H, Nevalainen T, Heikkila M, Tormala P, et al. The effect of an intramedullary carbon–fiber-reinforced liquid crystalline polymer implant on bone: an experimental study on rabbits. J Biomed Mater Res 1998;42:407–11.
[23] Ladizesky NH, Cheng YY, Chow TW, Ward IM. Acrylic resin reinforced with chopped high performance polyethylene fiber-properties and denture construction. Dent Mater 1993;9:128–35.
[24] Langer R, Vacanti JP. Tissue engineering. Science 1993;260:920–6.
[25] Laurencin CT, Ambrosio AMA, Borden MD, Cooper Jr JA. Tissue engineering: orthopedic applications. Annu Rev Biomed Eng 1999;1:19–46.
[26] Livingston T, Ducheyne P, Garino J. In vivo evaluation of a bioactive scaffold for bone tissue engineering. J Biomed Mater Res 2002;62:1–13.
[27] Ma PX, Zhang R, Xiao G, Franceschi R. Engineering new bone tissue in vitro on highly porous poly(α-hydroxyl acids)/hydroxyapatite composite scaffolds. J Biomed Mater Res 2001;54:284–93.
[28] Mikos AG, Bao Y, Cima LG, Ingber DE, Vacanti JP, Langer R. Preparation of poly(glycolic acid) bonded fiber structures for cell attachment and transplantation. J Biomed Mater Res 1993;27:183–9.
[29] Miyamoto Y, Ishikawa K, Takechi M, Toh T, Yuasa T, Nagayama M, et al. Histological and compositional evaluations of three types of calcium phosphate cements when implanted in subcutaneous tissue immediately after mixing. J Biomed Mater Res (Appl Biomater) 1999;48:36–42.
[30] Murphy WL, Kohn DH, Mooney DJ. Growth of continuous bonelike mineral within porous poly(lactide-*co*-glycolide) scaffolds in vitro. J Biomed Mater Res 2000;50:50–8.
[31] Piecuch JF, Goldberg AJ, Shastry CV. Compressive strength of implanted porous replamineform hydroxyapatite. J Biomed Mater Res 1984;18:39–45.
[32] Pourdeyhimi B, Wagner HD. Elastic and ultimate properties of acrylic bone cement reinforced with ultra-high-molecular-weight polyethylene fibers. J Biomed Mater Res 1989;23:63–80.
[33] Shindo ML, Costantino PD, Friedman CD, Chow LC. Facial skeletal augmentation using hydroxyapatite cement. Arch Otolaryngol Head Neck Surg 1993;119:185–90.
[34] Simon Jr CG, Khatri CA, Wight SA, Wang FW. Preliminary report on the biocompatibility of a moldable, resorbable, composite bone graft consisting of calcium phosphate cement and poly(lactide-*co*-glycolide) microspheres. J Orthop Res 2002;20:473–82.
[35] Simske SJ, Ayers RA, Bateman TA. Porous materials for bone engineering. Mater Sci Forum 1997;250:151–82.
[36] Sternberg SS. In: Histology for pathologists. New York, NY: Raven Press; 1992. p. 68–9.
[37] Suchanek W, Yoshimura M. Processing and properties of hydroxyapatite-based biomaterials for use as hard tissue replacement implants. J Mater Res 1998;13:94–117.
[38] Sugawara A, Chow LC, Takagi S, Chohayeb H. In vitro evaluation of the sealing ability of a calcium phosphate cement when used as a root canal sealer-filler. J Endodon 1990;16:162–5.
[39] Takagi S, Chow LC. Formation of macropores in calcium phosphate cement implants. J Mater Sci: Mater Med 2001;12:135–9.
[40] Tamai N, Myoui A, Tomita T, Nakase T, Tanaka J, Ochi T, et al. Novel hydroxyapatite ceramics with an interconnective porous structure exhibit superior osteoconduction in vivo. J Biomed Mater Res 2002;59:110–7.
[41] Taylor MS, Daniels AU, Andriano KP, Heller J. Six bioabsorbable polymers: in vitro acute toxicity of accumulated degradation products. J Appl Biomater 1994;5:151–7.
[42] Thomson RC, Yaszemski MJ, Powers JM, Mikos AG. Hydroxyapatite fiber reinforced poly (α-hydroxy ester) foams for bone regeneration. Biomaterials 1998;19:1935–43.
[43] Topoleski LDT, Ducheyne P, Cuckler JM. The effects of centrifugation and titanium fiber reinforcement on fatigue failure mechanisms in poly(methyl methacrylate) bone cement. J Biomed Mater Res 1995;29:299–307.
[44] Vallittu PK, Lassila VP, Lappalainen R. Transverse strength and fatigue of denture acrylic-glass fiber composite. Dent Mater 1994;10:116–21.
[45] von Gonten AS, Kelly JR, Antonucci JM. Load-bearing behavior of a simulated craniofacial structure fabricated from a hydroxyapatite cement and bioresorbable fiber-mesh. J Mater Sci: Mater Med 2000;11:95–100.
[46] Xu HHK, Eichmiller FC, Giuseppetti AA. Reinforcement of a self-setting calcium phosphate cement with different fibers. J Biomed Mater Res 2000;52:107–14.
[47] Xu HHK, Quinn JB. Calcium phosphate cement containing resorbable fibers for short-term reinforcement and macroporosity. Biomaterials 2002;23:193–202.
[48] Xu HHK, Quinn JB, Takagi S, Chow LC. Processing and properties of strong and non-rigid calcium phosphate cement. J Dent Res 2002;81:219–24.
[49] Xu HHK, Quinn JB, Takagi S, Chow LC, Eichmiller FC. Strong and macroporous calcium phosphate cement: effects of porosity and fiber reinforcement on mechanical properties. J Biomed Mater Res 2001;57:457–66.